High open-circuit voltage in perovskite solar cells

The role of hole transport layer

Ompong, David; Singh, Jai

Published in:
Organic Electronics

DOI:
10.1016/j.orgel.2018.09.006

Published: 01/12/2018

Document Version
Peer reviewed version

High Open-Circuit Voltage in Perovskite Solar Cells: The Role of Hole Transport Layer

David Ompong[1] and Jai Singh[1]

[1]*College of Engineering, IT and Environment, Charles Darwin University, 0909 Darwin, NT, Australia*

Abstract

Using the drift-diffusion model, a new expression for the open-circuit voltage (V_{oc}) in perovskite solar cells is derived. The V_{oc} increases with the ratio of the charge carrier mobilities (μ_e/μ_h) and by lowering the HOMO energy level of the hole transport layer (HTL). Using the derived V_{oc}, we have found an analytical expression for the bimolecular recombination coefficient which decreases exponentially with increasing temperature. We have shown that the recombination coefficient thus derived is reduced by the formation of polarons, which may be expected to increase the photocurrent and hence power conversion efficiency in perovskite solar cells.

Keywords:

Perovskite solar cells
Open-circuit voltage
Bimolecular recombination coefficient

1. Introduction

In recent years, organic-inorganic hybrid perovskite solar cells have attracted huge research interests due to the rapid increase in their power conversion efficiency (PCE) [1, 2], which is very promising for commercialization in the near future [3]. The semiconducting properties of all-inorganic metal halide perovskites have been studied since the 1950s [4]. It was reported in the 1980s [5] that the alloy PbI_2: KI had a direct band gap between 1.4 and 2.2 eV which matched with the peak of the sun's spectrum and hence was predicted to be a suitable material for photovoltaic applications. It was not until 2009 when Kojima *et al.* [6] first used organic-inorganic lead halide perovskites CH_3NH_3PbX (X = Br_3 or I_3) in dye-sensitized liquid junction-type solar cells which achieved an appreciable PCE of 3.8 % that much attention was paid to the development of solid state perovskite photovoltaics [7, 8]. Organo-metal halide perovskites have general formula ABX_3, where A is an organic cation, B is a divalent metal cation, and X is a monovalent halide anion [9]. In less than a decade the

efficiency of solar cells fabricated using such organo-metal halide perovskites as the active layer has increased from 3.8 % to more than 20 % [3, 9]. Perovskite materials have high absorption coefficient, direct band gap and absorption of photons generate free electron hole pairs or excitons with small binding energies. Perovskite materials also have moderate (compared to conventional inorganic semiconductors) [10] and balanced charge carrier mobility, long charge carrier diffusion length and lifetime, reduced recombination, and ambipolar transport properties [9, 11]. The above properties of perovskite materials make them unique materials for photovoltaic applications.

Although perovskite solar cells (PSCs) have achieved high PCE, the operation mechanism and device physics of PSCs are not yet clearly understood. To be able to further optimize the PCE of PSCs, it is important to gain a better understanding of material properties that influence the PCE [9, 11]. Also, as recombination leads to the loss of photogenerated charge carriers in solar cells, understanding the mechanism of recombination in PSCs and the V_{oc} related losses is needed in order to improve their photovoltaic performance [12-14].

One of the prominent photovoltaic parameters that has led to the high efficiency in PSCs is the open-circuit voltage (V_{oc}) and there is the need to understand the origins of the V_{oc} in PSCs [15]. The schematic layered structure of the perovskite solar cell considered in this study is shown in Fig. 1. For the structure given in Fig. 1, it is found that when an organic material with lower HOMO level is used as the hole transport layer (HTL) PSCs exhibit higher V_{oc} [7, 13, 15, 16].

In this work, we have derived an expression for V_{oc} for a hybrid heterojunction-like PSC with the structure TiO_2 (Electron transport layer)/perovskite/hole transport layers (HTLs) as shown in Fig. 1 by optimizing the drift-diffusion current density. The V_{oc} thus obtained

depends explicitly on the electron and hole mobility ratio, effective energy gap between the conduction band of the perovskite absorber and the HOMO energy level of the hole transport layer (HTL). An analytical expression is also derived for the temperature-dependent bimolecular recombination coefficient. The calculated values of both V_{oc} and the bimolecular recombination coefficient agree reasonably well with experimental results obtained in perovskite solar cells. The recombination expression shows that polaronic effects can help to reduced bimolecular recombination of charge carriers in perovskite solar cells.

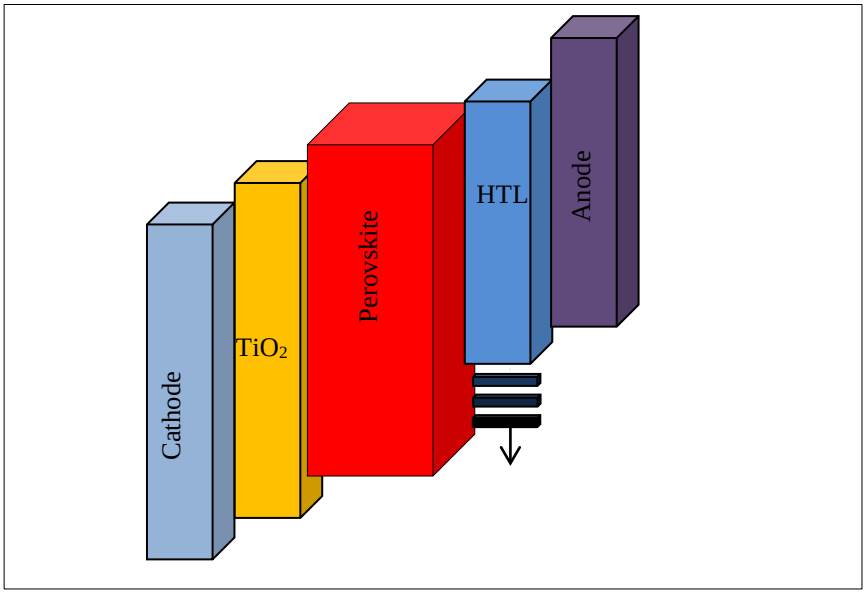

Figure 1 schematic structure of the PSCs studied in this work

2. Open-circuit voltage and bimolecular recombination coefficient of PSCs

Generally, the open-circuit voltage (V_{oc}) of an illuminated solar cell is defined by the energy difference between the quasi-Fermi level of the electron ($E_{F,e}$) in the electron extracting layer and the quasi-Fermi level of the hole ($E_{F,h}$) in the hole extracting layer as [17]:

$$-qV_{oc} = E_{F,e} - E_{F,h} \,, \tag{1}$$

where q is the charge of an electron. For PSCs, the V_{oc} can be written as [15]:

$$-qV_{oc} = E_g - \phi_n - \phi_p - \Delta E_{loss} \,, \tag{2}$$

where $\phi_n(\phi_p)$ is electron (hole) injection barrier height, ΔE_{loss} represents energy losses in transporting charge carriers to the electrodes. It has been observed that free charge carrier generation occurs at the interface between the perovskite and HTL via hole transfer from the perovskite to the HTL [2, 7, 16]. It may be noted that the energy alignment of electron transport layer (ETL) helps in the efficient transport of electrons from the perovskite layer to the cathode but the V_{oc} mainly depends on the energy difference between the conduction band edge of the perovskite active layer and the HOMO of the HTL [7, 13]. We have defined an effective band gap or an interface energy gap $E_g = |E_c - E_{HOMO}^{HTL}|$ between the energy of the conduction band edge (E_c) of the perovskite active layer and that of HOMO of the HTL (E_{HOMO}^{HTL}) [12, 18].

According to the drift-diffusion model the total current density *J* in a semiconductor under bias can be written as the sum of the electron and hole current densities, given by [19]:

$$J = J_n + J_p \,, \tag{3}$$

where $J_n = \mu_e n \nabla E_{F,e}$ is the electron current density and $J_p = \mu_h p \nabla E_{F,h}$ is the hole current density. Here n(p) is the electron (hole) concentration, $\mu_e(\mu_h)$ is the electron (hole) mobility, and $\nabla E_{F,e}(\nabla E_{F,h})$ is the gradient of the electron (hole) quasi-Fermi level. We have assumed that $\nabla E_{F,e} = \nabla E_{F,h}$ in this work. The total current density J in Eq. (3) can be expressed in terms of V_{oc}. The optimum J is thus obtained at a V_{oc} given by [12]:

$$V_{oc} = \frac{1}{q}\left\{E_g - 2\left(E_{F,h} - E_{HOMO}^{HTL}\right) + k_B T ln(P)\right\} \tag{4}$$

$$= \frac{1}{q}\left\{E_g - \Delta + \Phi\right\},$$

where $P = \frac{\mu_e}{\mu_h}$ is the ratio of electron-hole mobility [12], $\Delta = 2\left(E_{F,h} - E_{HOMO}^{HTL}\right)$ and $\Phi = k_B T ln(P)$. Under the condition of open-circuit voltage, i.e. when the charge generation rate G is equal to the recombination rate R, the open-circuit voltage in PSCs can written as [15]:

$$V_{oc} = \frac{1}{q}\left\{E_g - k_B T ln(\frac{\gamma N_c N_v}{G})\right\}, \quad (5)$$

where γ is material dependent bimolecular recombination coefficient, T is temperature, ε is the static dielectric constant, ε_o is absolute permittivity, k_B is Boltzmann's constant, $N_c(N_v)$ is the concentration of electrons at the band edge of the perovskite conduction band (concentration of holes at the HTL HOMO energy level). It is assumed that $N_c = N_v = N$. From Eq. (4) and Eq. (5), the temperature-dependent bimolecular recombination constant γ can be obtained as:

$$\gamma = \frac{G}{N^2 P} e^{2(E_{F,h} - E_{HOMO}^{HTL})/k_B T} . \quad (6)$$

It may be noted here that in most perovskites only the bimolecular recombination plays important role. This is because monomolecular recombination has relatively small or negligible impact on the performance of PSCs due to the absence of trapping in perovskites [1, 20] even at low charge carrier densities where trap-assisted monomolecular recombination is expected to dominate [20]. Also the third order Auger recombination is known to have relatively little importance in perovskites [21].

3. Results and discussions

The V_{oc} of a solar cell is generated by the build-up of electrons in the n-type material and holes in the p-type material, resulting in the splitting of the quasi-Fermi levels for electrons and holes [2]. Using Eq. (4), we have calculated V_{oc} for a few PSCs with different perovskite

materials and HTLs listed in table 1, along with the corresponding experimental results for comparison. According to Eq. (4), V_{oc} of PSCs depend on three terms. The first is the effective band gap E_g which can be changed by changing the perovskite material and the HTL as shown in table 1. The second term Δ reduces with the increase of the hole concentration in the perovskite because for higher hole concentration the hole quasi-Fermi level $E_{F,h}$ moves closer to the HOMO level E_{HTL}^{HOMO} of the HTL. This is what occurs in the case of PSCs which have high charge carrier concentrations due to the low recombination rate, the hole quasi-Fermi level moves much closer to the HOMO energy level of the HTL which reduces the second term in Eq. (4) resulting in higher V_{oc}. The third term of Eq. (4), which is the transport term also has small contribution compared to the energetic terms because of the logarithmic dependence on P. Therefore, PSCs have higher V_{oc} because of the reduced loss in second term of Eq. (4) and this is what has been observed experimentally, that is, using HTL which has lower HOMO in relation to the vacuum level increases V_{oc} [7, 13, 16]. This implies that the high V_{oc} is due to intrinsic properties of the PSC materials such as the low recombination rate, high charge carrier concentration and ambipolar transport properties coupled with the low-lying HOMO level of the HTL [13, 22]. This agrees with the experimental results that low-lying HOMOs give higher V_{oc} as it can be seen in table 1. This may also lead one to conclude that the recombination between electrons and holes within the perovskite active layer is slower than that between electrons in perovskite and holes in HTL across the perovskite-HTL interface [16]. Also, the perovskite-ETL interface plays a less dominant role in influencing charge carrier recombination in PSCs [23].

In table 1, the calculated V_{oc} from Eq. (4) for perovskite and $PC_{61}BM$ HTL combination is 1.71 eV, which much larger than the 1.06 eV measured experimentally. We calculated the interface energy gap E_g from [13]. Using this E_g in Eq. (4), one gets V_{oc} of 1.71 eV. However, the HOMO energy level of $PC_{61}BM$ is found to be varying from -5.6 eV [24] to -

6.5 eV [13] in the literature. This corresponds to V_{oc} ranging from 1.21 V to 1.71 V, assuming all the other terms remain the same in Eq. (4). Thus, the discrepancy in the calculated and experimental V_{oc} may be attributed to the wide range of values of $PC_{61}BM$ HOMO level. A similar argument can be made for the discrepancy in V_{oc} of the last three HTLs in table 1. It can be noted that the conduction band edge of $CH_3NH_3PbBr_3$ reported in [7] is 0.82 eV bigger than what is reported in [13]. Figure 2 shows the energy level diagram of the perovskite materials and the HTLs that we studied in this work.

Table 1. Calculated results of V_{oc} from Eq. (4) for three different perovskite materials with several materials selected for HTL using the electron mobility in the perovskite as 100 $cm^2/(V.s)$[10]. Also, with $p = \times 10^{18}$ cm^{-3}, $N = \times 10^{21}$ cm^{-3}, and $k_BT = 26$ meV [15] we estimate $\Delta = 0.36$ eV using $p = Ne^{\Delta/2k_BT}$. The experimental results are also given for comparison.

Perovskite material	E_c (eV)	HTL	E_{HOMO}^{HTL} (eV)	E_g (eV)	Φ (eV)	V_{oc}^{calc} (V)	V_{oc}^{expt} (V)	Ref.
$CH(NH_2)_2PbBr_3$	-3.90	S-O	-5.22	1.32	0.40	1.36	1.47	[16]
	-3.90	SO7	-5.41	1.51	0.05	1.47	1.50	[16]
	-3.90	SO8	-5.31	1.41	0.05	1.10	1.43	[16]
	-3.90	SO9	-5.31	1.41	0.05	1.10	1.46	[16]
	-3.90	SO10	-5.33	1.43	0.05	1.12	1.47	[16]
$CH_3NH_3PbBr_3$	-4.20	P3HT	-5.10	0.90	0.18	0.72	0.84	[13]
	-4.20	TPD	-5.30	1.10	0.30	1.05	1.20	[13]
	-4.20	$PC_{61}BM$	-6.10	1.90	0.17	1.71	1.06	[13]
	-4.20	PDI	-5.80	1.60	0.10	1.34	1.30	[13]
$CH_3NH_3PbBr_3$	-3.38	PTAA	-5.14	1.76	0.26	1.66	1.29	[7]
	-3.38	PF8-TAA	-5.44	2.06	0.22	1.92	1.36	[7]
	-3.38	PIF8-TAA	-5.51	2.13	0.20	1.97	1.40	[7]

P3HT: poly(3-hexyl)thiophene

$PC_{61}BM$: [6,6]-phenyl-C_{61}-butyric acid methyl ester

PDI: N,N′ -dialkyl perylenediimide

PTAA: N-(4-bromophenyl)-4-(4,4,5,5-tetramethyl-1,3,2-dioxaborolan-2-yl)-N-(2,4-dimethyl-phenyl)benzenamine

PF8TAA: poly(9,9-dioctylfluorene-*alt*-4-*sec*-butylphenyldiphenylamine)

PIF8-TAA: Polyindenofluoren-8-triarylamine

SO7- SO10: fluorene−dithiophene derivatives with different structural modifications

Spiro-OMeTAD (S-O): 2,2′,7,7′-Tetrakis-N,N-p dimethoxyphenylamino)-9,9′- spirobifluorene

TAA: Triarylamine

TPD: N,N′ -bis(3-methylphenyl)-N,N′ -diphenylbenzidine

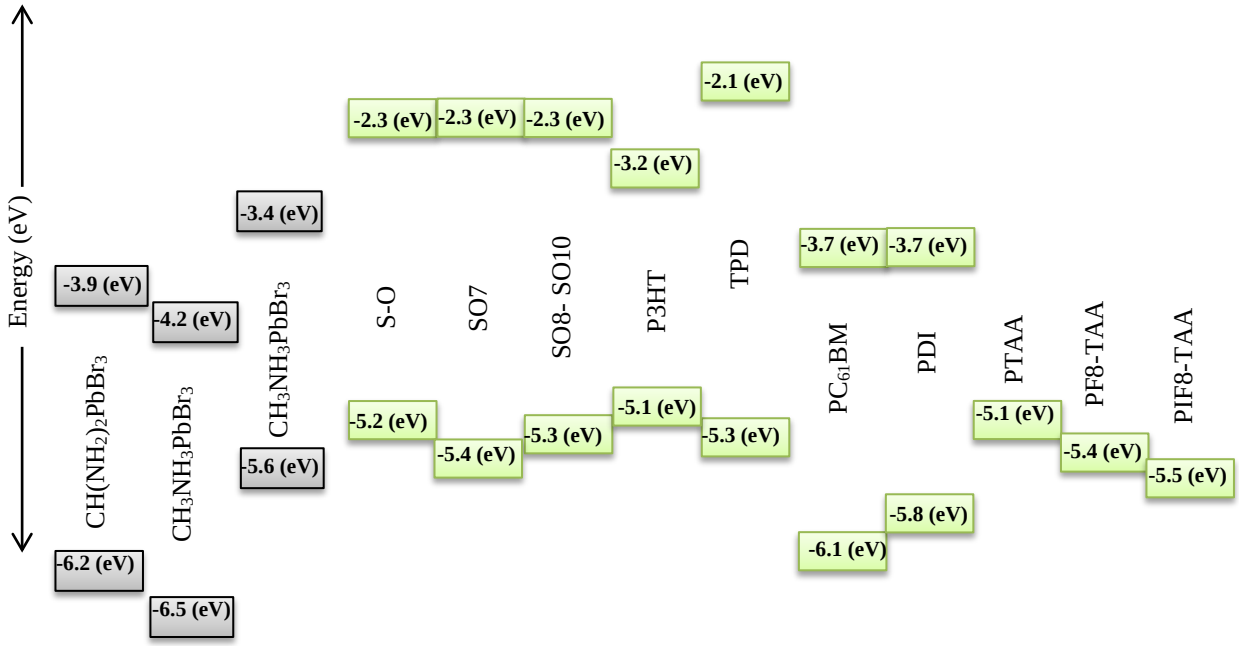

Figure 2 shows the energy level diagram of the perovskite materials and the HTLs found in table 1.

Having discussed the influence of Δ on V_{oc} , we now consider the effect of the third term Φ. When $\mu_e \sim \mu_h \sim \mu$ then $\ln P \sim 0$ and the V_{oc} will become temperature independent. However if $\mu_e \neq \mu_h$ then V_{oc} increases with P as shown in Fig. 3. Oga *et. al.* [25], have used different perovskite preparation methods which resulted in different mobilities for electrons and holes. Using these mobilities, for PSCs with the perovskite deposited on TiO_2 we have found P=0.03, which gives a smaller $V_{oc} = 0.91$ V compared to the perovskite deposited on

Al_2O_3 which gave P=0.43 and $V_{oc} = 0.98$ V. These results calculated using Eq. (4) agree with those of Oga *et al*.[25] as shown in their Fig. 3 of the supporting information.

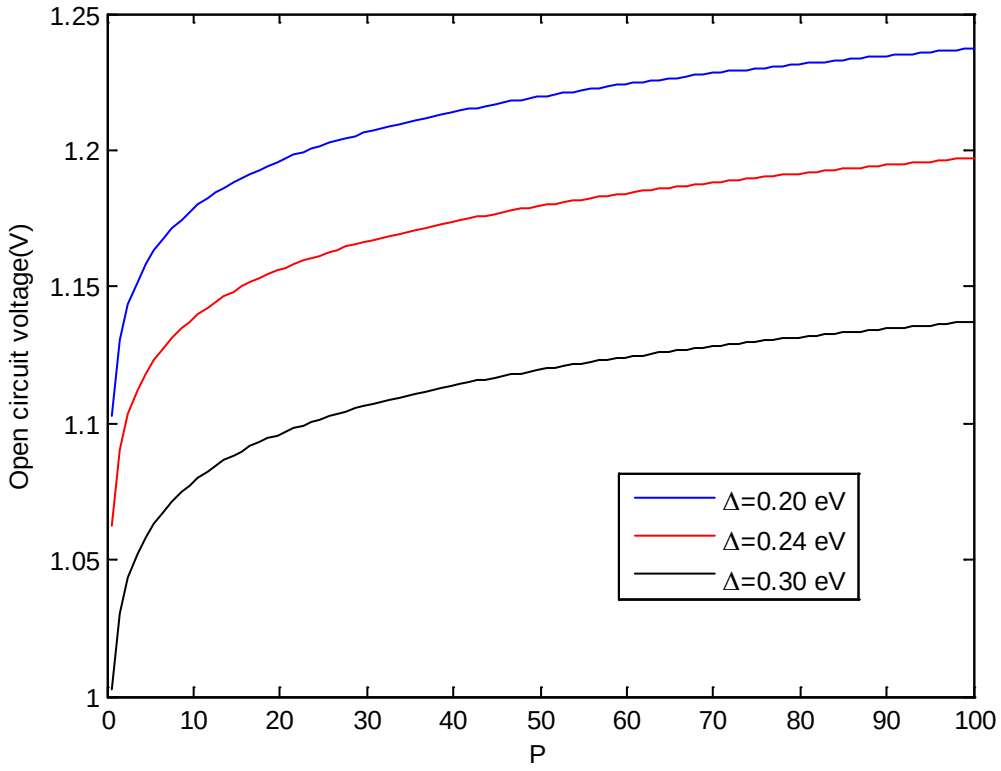

Figure 3. The V_{oc} in Eq. (4) plotted as a function of P for three different values of Δ, $E_g = 1.32$ eV.

For studying the significance of bimolecular recombination in PSCs, we consider Eq. (6). The bimolecular recombination can be regarded as both non-radiative and radiative. Theoretical models which consider bimolecular recombination to be radiative give better agreement with experimental results [1]. The bimolecular recombination derived using van Roosbroeck–Shockley's theory is based on the principle of detailed balance of the system's properties in thermal equilibrium, and depends on the product of individual electron and hole concentrations [1, 26]. In the detailed balance, it is the rate of thermally generated charge carriers (in the dark) but not that of the photo-generated ones that must be equal to the recombination rate at thermal equilibrium [27].

With $N = 2(2\pi m^* k_b T/h^2)^{\frac{3}{2}}$ [28] we get from Eq. (6) $\gamma \sim (m^*)^{-3}$ at any constant temperature. Here m^* is charge carrier effective mass and h is Planck's constant. However, in a polaronic form the effective mass m^* becomes heavier [29] leading to a drastic reduction in γ. This is in agreement with the results obtained in Ref. [1]. Thus, if charge carriers in lead halide perovskites form polarons as suggested [30-32] then the recombination rate of charge carriers is expected to reduce, leading to a better performance in PSCs.

In Fig. 4, we have plotted γ as a function of temperature T (blue solid line) using $G = 1.2 \times 10^{22}$ cm^{-3}s^{-1}, $N^2 = 9 \times 10^{32}$ cm^{-6}, $P = 0.005$, and $\Delta = 0.01$ eV. The experimental points (red squares) are obtained from [32]. In calculating γ in Fig. 4, we have assumed that the ratio of charge carrier mobility P and $E_{F,h}$ are temperature independent.

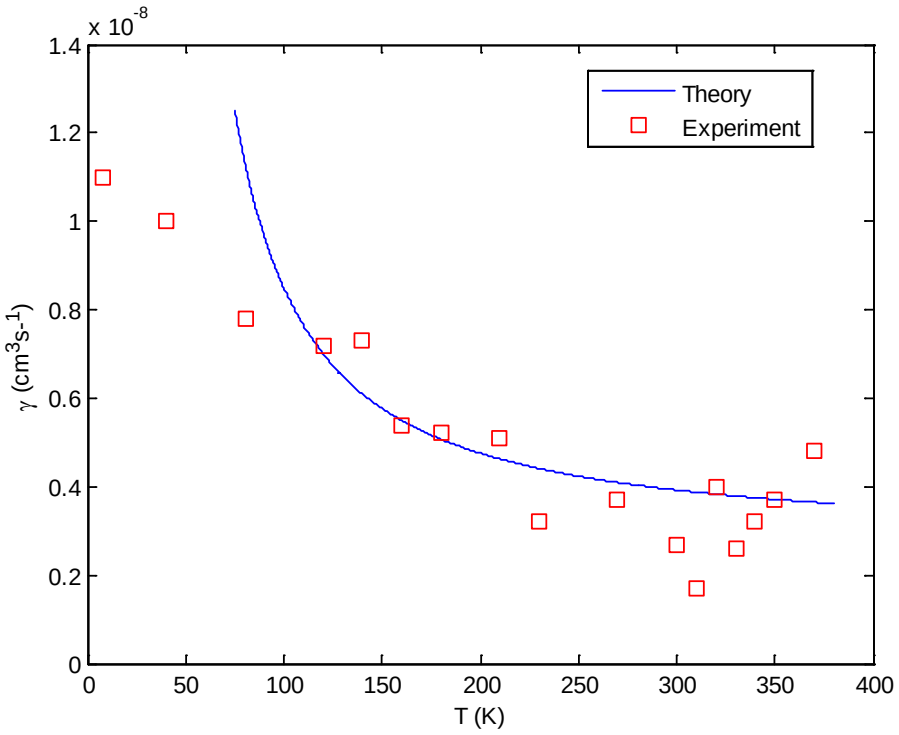

Figure 4. Experimental bimolecular recombination coefficient (red squares) as a function of temperature from Ref. [32]. The blue solid line represents the theoretical temperature dependence of γ calculated using Eq. (6).

It can be seen from Fig. 4 that the calculated results agree reasonably well with experimental results in the whole temperature range. Both the theoretical and experimental bimolecular recombination coefficients increase as temperature decreases. This may be attributed to the less likelihood of formation of polarons in the low temperature range due to the organo-metal halide perovskites being in orthorhombic phase (below ~100 K) where the molecular dipoles are frozen. The perovskite attains a tetragonal phase in the intermediate temperature range and cubic phase in the high temperature range. In both of these phases the molecular dipoles attain increasing rotational freedom with increasing temperature [31, 32] and hence enhanced formation of polarons [20], leading to lower recombination rate as shown in Fig. 4. The theoretical and experimental results shown Fig. 4 illustrate that γ decreases as the temperature increases. This is not in agreement with the calculated results in [33] where γ is shown to increase with temperature. This discrepancy may be attributed to the fact that in [33] γ is calculated in the reciprocal space.

4. Conclusions

We have derived V_{oc} for PSCs which is independent of the injection barrier contact potential but depends on the charge carrier mobility ratio. The higher V_{oc} found in PSCs is attributed to the fact that energetic and transport losses are small due to their unique and intrinsic optical and electronic properties. Using HTL with lower HOMO level yields higher V_{oc} and the formation of polarons may help to reduced bimolecular recombination. Our results are expected to assist in optimization of PCEs of PSCs.

References

[1] Y. Chen, H. T. Yi, X. Wu, R. Haroldson, Y. N. Gartstein, Y. I. Rodionov, K. S. Tikhonov, A. Zakhidov, X. Y. Zhu and V. Podzorov, Nat. Comm. **7**, 12253 (2016).

[2] M. M. Lee, J. Teuscher, T. Miyasaka, T. N. Murakami and H. J. Snaith, Science, **338**, 643 (2012).

[3] L. K. Ono, N.-G. Park, K. Zhu, W. Huang and Y. Qi, ACS Energy Lett. **2**, 1749 (2017).

[4] L. D. Whalley, J. M. Frost, Y.-K. Jung and A. Walsh, J. Chem. Phys. **146**, 220901 (2017).

[5] A. M. Salau, Sol. Energy Mater. **2**, 327 (1980).

[6] A. Kojima, K. Teshima, Y. Shirai and T. Miyasaka, J. Am. Chem. Soc. **131**, 6050 (2009).

[7] S. Ryu, J. H. Noh, N. J. Jeon, Y. Chan Kim, W. S. Yang, J. Seo and S. I. Seok, Energy & Environ. Science **7**, 2614 (2014).

[8] C. Barugkin, J. Cong, T. Duong, S. Rahman, H. T. Nguyen, D. Macdonald, T. P. White and K. R. Catchpole, J. Phys. Chem. Lett. **6**, 767 (2015).

[9] Z. Song, S. C. Watthage, A. B. Phillips and M. J. Heben, J. Photon. Energy **6**, 022001 (2016).

[10] T. M. Brenner, D. A. Egger, A. M. Rappe, L. Kronik, G. Hodes and D. Cahen, J. Phys. Chem. Lett. **6**, 4754 (2015).

[11] S. Dong, Y. Liu, Z. Hong, E. Yao, P. Sun, L. Meng, Y. Lin, J. Huang, G. Li and Y. Yang, Nano Lett. **17**, 5140 (2017).

[12] D. Ompong and J. Singh, Front. Nanosci. Nanotech. **2**, 43 (2016).

[13] E. Edri, S. Kirmayer, D. Cahen and G. Hodes, J. Phys. Chem. Lett. **4**, 897 (2013).

[14] B. Suarez, V. Gonzalez-Pedro, T. S. Ripolles, R. S. Sanchez, L. Otero and I. Mora-Sero, J. Phys. Chem. Lett. **5**, 1628 (2014).

[15] W. Yang, Y. Yao and C.-Q. Wu, J. Appl. Phys. **117**, 095502 (2015).

[16] N. Arora, S. Orlandi, M. I. Dar, S. Aghazada, G. Jacopin, M. Cavazzini, E. Mosconi, P. Gratia, F. De Angelis, G. Pozzi, M. Graetzel and M. K. Nazeeruddin, ACS Energy Lett. **1**, 107 (2016).

[17] B. A. Gregg, J. Phys. Chem. B **107**, 4688 (2003).

[18] G. Garcia-Belmonte and J. Bisquert, Appl. Phy. Lett. **96**, 113301 (2010).

[19] J. Nelson, *The Physics of Solar Cells* (Imperial College Press, London, 2003).

[20] F. Ambrosio, J. Wiktor, F. De Angelis and A. Pasquarello, Energy & Environ. Science, **11**, 101 (2018).

[21] M. B. Johnston and L. M. Herz, Acc. Chem. Res. **49**, 146 (2016).

[22] W. S. Yang, J. H. Noh, N. J. Jeon, Y. C. Kim, S. Ryu, J. Seo and S. I. Seok, Science, **348**, 1234 (2015).

[23] W. Tress, M. Yavari, K. Domanski, P. Yadav, B. Niesen, J. P. Correa Baena, A. Hagfeldt, and M. Graetzel, Energy & Environ. Science. **11**, 151 (2018).

[24] G. Ren, C. W. Schlenker, E. Ahmed, S. Subramaniyan, S. Olthof, A. Kahn, D. S. Ginger, and S. A. Jenekhe, Adv. Funct. Mater. **23**, 1238 (2013).

[25] H. Oga, A. Saeki, Y. Ogomi, S. Hayase and S. Seki, J. Am. Chem. Soc. **136**, 13818 (2014).

[26] J. Singh, *Optical Properties of Condensed Matter and Applications*, 1st Ed. (Wiley, England, 2006).

[27] J. C. Blakesley and D. Neher, Phys. Rev. B **84**, 075210 (2011).

[28] T. S. Sherkar and L. Jan Anton Koster, Phys. Chem. Chem. Phys. **18**, 331 (2016).

[29] J. Singh and K. Shimakawa, *Advances in amorphous semiconductors*. (Taylor & Francis, London, 2003).

[30] H. Zhu, K. Miyata, Y. Fu, J. Wang, P. P. Joshi, D. Niesner, K. W. Williams, S. Jin and X.-Y. Zhu, Science **353**, 1409 (2016).

[31] M. Bonn, K. Miyata, E. Hendry and X. Y. Zhu, ACS Energy Lett. **2**, 2555 (2017).

[32] R. L. Milot, G. E. Eperon, H. J. Snaith, M. B. Johnston and L. M. Herz, Adv. Func. Mater. **25**, 6218 (2015).

[33] P. Azarhoosh, S. McKechnie, J. M. Frost, A. Walsh, and M. v. Schilfgaarde, APL. Mater. **4**, 091501 (2016).